BOREAL ENVIRONMENT RESEARCH 18: 280–302
ISSN 1239-6095 (print) ISSN 1797-2469 (online)

Helsinki 28 June 2013

Air pollution episodes in Stockholm regional background air due to sources in Europe and their effects on human population

Oskar Jönsson[1)2)], Camilla Andersson[1)*], Bertil Forsberg[3)] and Christer Johansson[2)4)]

[1)] *Swedish Meteorological and Hydrological Institute, SE-601 76 Norrköping, Sweden (*corresponding author's e-mail: camilla.andersson@smhi.se)*
[2)] *Department of Applied Environmental Science, SE-106 91 Stockholm University, Sweden*
[3)] *Occupational and Environmental Medicine, SE-901 87 Umeå University, Sweden*
[4)] *Environment and Health Administration, P.O. Box 8136, SE-104 20 Stockholm, Sweden*

Received 29 Mar. 2012, final version received 31 Aug. 2012, accepted 31 July 2012

Jönsson, O., Andersson, C., Forsberg, B. & Johansson, C. 2013: Air pollution episodes in Stockholm regional background air due to sources in Europe and their effects on human population. *Boreal Env. Res.* 18: 280–302.

Using air quality measurements, we categorized air pollution according to source sectors in a rural background environment in southern Sweden based on hourly air-mass backward trajectories during 1997–2010. Concentrations of fine ($PM_{2.5}$) and sum of fine and coarse particulate matter (PM_{10}), accumulation mode particle number, black carbon and surface ozone were 4.0, 3.9, 4.5, 6.8 and 1.3 times higher, respectively, in air masses from the southeast as compared with those in air masses from the cleanest sector in the northwest, consistent with air-mass transport over areas with relatively high emissions of primary particulate matter (PM) and secondary PM precursors. The highest ultrafine particle numbers were associated with clean air from the northwest. We estimate that almost 7.8% and 0.6% higher premature human mortality is caused by $PM_{2.5}$ and ozone exposure, respectively, when air originates from the southeast as compared with that when air originates from the northwest. Reductions of emissions in eastern Europe would reduce the highest air pollution concentrations and associated health risks. However, since air masses from the southwest are more frequent, emissions in the western part of Europe are more important for annual mean premature mortality.

Introduction

Long-range transport of air pollution has been addressed scientifically for policy negotiations since 1979 by the Convention on Long-range Trans-boundary Air Pollution (CLRTAP). The convention was formed as a result of the realisation that long-range transport is important for air quality and deposition of acidifying and eutrophying pollutants (e.g. Rodhe 1972, Eliassen 1978). Pollutants such as fine particulate matter ($PM_{2.5}$), black carbon (BC) and surface ozone, have lifetimes of days or even weeks, i.e. long enough for them to be transported up to thousands of kilometers. For these pollutants, long-range transport make an important contribution,

Editor in charge of this article: Hannele Korhonen

increasing the long-term mean concentration as well as causing episodic periods with extraordinary high concentrations (Areskoug *et al*. 2000). Exposure to PM can lead to reduced life expectancy due to pulmonary and cardiovascular diseases (Pope and Dockery 2006, WHO 2006). Forsberg *et al*. (2005) estimated 3500 premature human deaths, corresponding to a reduced life expectancy of seven months, due to long-range transported PM in Sweden. Surface ozone causes respiratory problems and may increase risks of premature human mortality (WHO 2008). It also causes damages to vegetation (Krupa and Manning 1988). European anthropogenic emissions of air pollutants and its precursors have decreased since the 1990s (e.g. EMEP 2011a) as a result of policy actions, likely causing the observed downward tendency measured in PM at EMEP (European Monitoring and Evaluation Programme) stations (EMEP 2011b). However, the measurement sites with long enough PM records are sparse; only four EMEP sites have reported PM data back to 1997 (EMEP 2011b).

Knowledge on the importance of different source sectors or regions is necessary for taking appropriate actions to reduce emissions. Under the CLRTAP convention, the EMEP chemistry transport model is used to assess source contributions for various pollutants and many other similar models exist as described by Kukkonen *et al*. (2012). However, there are many gaps in our knowledge, especially for aerosols, that make such assessments uncertain (Andersson *et al*. 2009, Kulmala *et al*. 2009). This involves all steps in modelling: emissions, atmospheric transport and deposition, as well as photochemical and aerosol dynamic processes including gas-particle transformation. Uncertainties are particularly large for certain particle properties such as particle number concentrations.

A complementary approach is to use *in-situ* measured rural background concentrations of air pollutants in combination with air-mass backward trajectory analyses to assess the origin of long-range transported air pollution (e.g. Abdalmogith and Harrison 2005, Lee *et al*. 2006, Forsström *et al*. 2009, Fleming *et al*. 2012). The advantage is that this does not require any information on the emissions and no chemical or aerosol process modelling.

In this study, we use air-mass backward trajectories to assess the contribution of four source regions in Europe (southwest, southeast, northwest and northeast) to the concentrations of particulate matter (PM_{10}, $PM_{2.5}$), particle number (PN), BC and surface ozone in the area around Stockholm, Sweden. We estimate the uncertainties involved in trajectory modelling by sensitivity analyses, relate our results to current emission estimates and we also estimate the relative roles of the source regions on premature human mortality associated with $PM_{2.5}$ and ozone.

Methods

Site description and observational methods

We used hourly mean concentrations of surface ozone, $PM_{2.5}$, PM_{10}, BC, and particle number (in particle diameter range 10–451 nm) from the measurement site Aspvreten (*see* Fig. 1a). Aspvreten is a regional air quality monitoring station, positioned at 58.80°N and 17.38°E. The station is situated about two kilometers inland from the coastline in a rural area vegetated by mixed coniferous and deciduous forest with a few meadows. The influence from anthropogenic activities is small, as the closest large metropolitan area is Stockholm (ca. 70 km towards the northeast), and the area around the station is sparsely populated. The station is operated by the Atmospheric Science Unit of the Department of Applied Environmental Science at Stockholm University, and is a part of the EMEP network as well as the EUSAAR network (European Supersites for Atmospheric Aerosol Research; Philipin *et al*. 2009). The analysis spans the period 1997–2010, however due to data availability restrictions (*see* Appendix 1) only surface ozone was analysed for the full period. For the other pollutants the analysed periods were PM_{10}: 1997–2009, $PM_{2.5}$: 1998–2010, particle number: 2000–2010, and BC: 2004–2010.

Details on the measurement methods are described in Areskoug *et al*. (2000) and Krecl *et al*. (2011) for PM and BC, and in Tunved *et al*. (2003) for PN. The reference method SS-EN 14625:2005 was used for surface ozone. PM

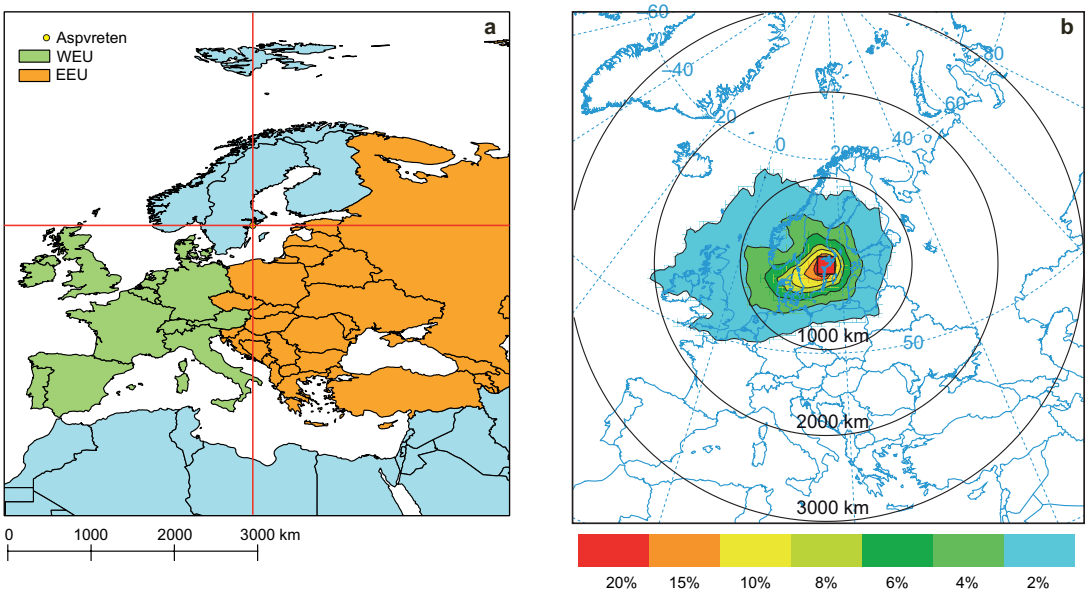

Fig. 1. (**a**) Map of Europe showing the four sectors, and eastern (EEU) and western (WEU) Europe. (**b**) Geographic distribution of all trajectories for the period 1997–2010.

measurements were corrected for the loss of volatile material due to the heating with the use of a correction factor, as described in Krecl *et al*. (2011). Particle number concentrations were divided into two size fractions: ultra-fine (nucleation and Aitken modes) with mobility diameters between 10 and 110 nm (PN_{UF}), and accumulation mode diameters between 113 and 451 nm (PN_A).

For ozone, we calculated the daily maximum eight-hour mean concentration using a 75% data requirement in each eight-hour period for calculating the running mean. For the other air pollutants, daily mean concentrations were formed with a 75% data requirement each day. These metrics are used in the current legislation, and our choice gave us the opportunity to define high levels as the levels exceeding legislated thresholds. For surface ozone, we used the surface ozone target value of 120 μg m^{-3} as a threshold to define high ozone concentration days. This resulted in 111 days total during 1997–2010. Since ozone can be transported downward from the stratosphere, the 111 highest ozone days were divided into two classes: "high altitude" if their daily eight-hour mean trajectory had reached above 2000 m and "low altitude" when the trajectory had remained below 2000 m. In addition, we selected for each of the other pollutants 111 days that showed the highest concentrations in order to obtain as large a dataset as for surface ozone. The air mass origin of these 111 days were analysed in more detail. The lowest concentration for each of the pollutants in the 111-day data sets resulted in thresholds for high concentration days as follows: $PM_{10} > 27$ μg m^{-3}, $PM_{2.5} > 22$ μg m^{-3}, $PN_{UF} > 3681$ N cm^{-3}, $PN_A > 1643$ N cm^{-3} and BC > 0.85 μg m^{-3}.

Trajectory modelling

Using the model HYSPLIT (HYbrid Single-Particle Lagrangian Integrated Trajectory) (Draxler and Hess 1998) version 4, we calculated three-dimensional five-day air-mass backward trajectories starting at Aspvreten (Fig. 1) every hour for the period 1997–2010. Three-dimensional trajectories modelled using both horizontal and vertical wind components are considered the most accurate (Stohl 1998). Five days is long enough to represent transport from sources across Europe. This is also on the order of the residence time of the air pollutants studied, although for hemispheric background ozone and accumulation mode particles the residence time

may be longer, even up to weeks. This means that the air-mass backward trajectories and subsequent air-pollutant classification will represent air pollution originating from across Europe. A longer modelling time-scale than five days is not desirable as trajectory errors increase with travelled distances (Stohl 1998).

We used modelled meteorological wind fields from two data sets to calculate the air-mass backward trajectories. The datasets were FNL ("Final run", covering the years from 1997 to 2005) and GDAS (Global Data Assimilation System, covering the years from 2005 onwards). Both were produced by the National Centers for Environmental Prediction (NCEP). FNL consist of archived six-hourly data with spatial resolution of 129 × 129 polar stereographic grids and 13 vertical levels ranging from 20 to 1000 hPa. In GDAS, the resolution is three hours with a 1° latitude/longitude grids and with 23 vertical levels ranging from 20 to 1000 hPa. The coarser resolution of the FNL data could cause greater interpolation errors. Therefore, we conducted a sensitivity analysis between the two datasets for the overlapping year 2005. The analysis shows only minor differences in source region mean concentrations (*see* Appendix 2) and therefore we chose to include both datasets in order to cover the entire time period from 1997 to 2010, using GDAS for 2005.

Modelled trajectories are only an estimation of the transport of a single particle (Stohl 1998), but they are useful for identifying potential source or receiver areas (Dvorská *et al*. 2009). Uncertainties of modelled trajectories include truncation, interpolation, starting position errors, and the most common and largest errors arising from uncertainties in horizontal and vertical wind (Stohl 1998). While the measurements were taken close to the surface, the starting height of the air mass backward trajectory should be set higher up in the atmospheric boundary layer in order to avoid that the model results are affected by surface friction. The optimal starting height for each modelling situation is dependent on climatic and geographic conditions, and thus the ideal starting height varies (Lee and Ashbaugh 2007). In this study, we used the arrival starting height of 100 m, which should be representative for long-range transport of the air measured. This starting height has previously been used in trajectory modelling in Sweden and Scandinavia, e.g. by Tunved *et al*. (2010). Trajectories can be very different depending on the chosen starting height, and ensemble methods, where multiple trajectories are calculated using different starting heights, can be used to estimate the starting position errors (Stohl 1998). In Appendix 2, we present sensitivities to plausible starting heights and other factors.

Sector based source classification

We chose to classify the trajectories into four sectors with an origin at Aspvreten, divided by straight longitudinal and latitudinal lines intersecting the site (Fig. 1a). The source sector of the daily maximum eight-hour mean ozone was derived from a mean trajectory over the eight hours that gave rise to the daily maximum value. For the other pollutants, the hourly air-mass backward trajectories were used in the classification. If the eight-hour mean or hourly trajectories remained in one sector for at least 80% of the time throughout the five days, it was assigned to that sector, otherwise it was assigned to a separate multisector group. We formed the eight-hour mean trajectories using the HYSPLIT trajmerge function with the 75% data requirement. We analysed all hours of the year for all air pollutants except for ozone, which has a strong seasonal variation, hence, for ozone we also analyzed the period March–September, i.e. the part of the year with the highest concentrations.

Premature human mortality estimation

Using pollutant-specific risk coefficients, we estimated the increased premature human mortality due to exposure to increased mean $PM_{2.5}$ and ozone concentrations for each of the source regions including the multisector group. The long-term effect of particles in ambient air on human mortality (hereafter referred to as mortality) is scientifically established only for $PM_{2.5}$. The baseline for $PM_{2.5}$ was set at the annual mean concentration of the cleanest sector, and premature mortality was calculated based on

the levels above that value in the other sectors. This gives the increased mortality associated with the elevated pollutant concentrations as compared with that for the cleanest air mass. We also estimated the increased mortality over the whole period considering the proportion of total days with air masses arriving from each source region. The mean value in the northwestern sector, 4.4 μg m^{-3}, likely represents mainly natural-source contributions (as discussed by Forsberg *et al*. 2005). This value is lower than the WHO annual guideline value for $PM_{2.5}$ (10 μg m^{-3}), but as stated by WHO (2006) research has not identified any threshold below which adverse effects do not occur, so the WHO guideline value is not a limit below which there are no health effects. The WHO annual guideline was exceeded only in the southeastern sector. There is also a WHO guideline for a 24-hour mean value (25 μg m^{-3}), which is rarely exceeded at this site.

For $PM_{2.5}$, we used 6% increase in premature mortality per 10 μg m^{-3} increase in annual mean $PM_{2.5}$ (Pope *et al*. 2002). This association comes from a study of long-term effects. For estimating the effect of ozone, we used 0.33% (95% confidence limits = 0.17%–0.52%) increase in daily number of human deaths per 10 μg m^{-3} increase in daily maximum eight-hour mean ozone concentration. This coefficient is based on effects calculated in the European APHEA-2 study using the daily maximum one-hour means (Gryparis *et al*. 2004). In the same study, the increase was 0.31%–0.34% in two meta-regression models using the daily maximum eight-hour mean.

Results

Influence of source region on concentrations

A large proportion of the observed concentrations, classified by source region, were assigned to the multisector, however the remaining data still includes more than 4500 hours in each sector for the PM and PN fractions (Table 1 and Fig. 2). For BC, the lowest number of hours was 2500 in the southeastern sector (*see* Table 1 and Fig. 2). The highest mean concentrations for most pollutants were observed in air originating from the southeast and the lowest in air from the northwest: the mean values of PM_{10}, $PM_{2.5}$, PN_A, BC and surface ozone were 4, 3.9, 4.5, 6.8 and 1.3 times higher, respectively, in air from the southeast than in air from the northwest. For PN_{UF}, the highest mean concentrations — 1.7 times higher than the lowest concentration observed from the southeast — originated from the northwest, and highest maximum concentrations from the southwest. The relative differences between the sectors were lowest for surface ozone and PN_{UF}.

Particulate matter (PM_{10} and $PM_{2.5}$)

The overall PM_{10} mean concentration for the studied period was 10.8 μg m^{-3}, and for $PM_{2.5}$ 8.0 μg m^{-3}. Air from the southeast had the highest PM_{10} and $PM_{2.5}$ concentrations, with the means of 22.9 μg m^{-3} and 17.2 μg m^{-3}, respectively. These were about twice as high as the means from the southwest, which was the second highest source region. Air from the southeast also differed from all the other source regions by having fewer hours of low concentrations and a higher proportion of very high concentrations.

Particle number, accumulation mode (PN_A, 0.11–0.45 μm diameter)

The overall annual mean for the period 2001 to 2009 (years with > 50% data capture) was 590 N cm^{-3}. The highest mean PN_A number (1180 N cm^{-3}) was associated with air masses from the southeast. This is about 1.9 times higher than the second highest mean, which was observed in air masses from the southwest.

Particle number, ultrafine mode (PN_{UF}, < 0.1 μm)

The annual mean for the period 2001–2009 (years with > 50% data capture) was 1720 N cm^{-3}. The highest mean PN_{UF} number (2190 N cm^{-3}) was, in contrast to all other pollutants, measured in air transported from the northwest.

This mean was 1.2 times higher than the mean in air masses from the second highest sector, the southwest.

Black carbon (BC)

The mean BC concentration at Aspvreten during the period 2005–2010 (years with > 50% data capture) was 0.32 μg m^{-3}. As for PM, the highest mean concentration, 0.88 μg m^{-3}, was associated with air transported from the southeast. This is about 2.5 times as high as the mean from the southwest, which was the source region with the second highest mean concentration. Air from the north had lower mean concentration than air from the south.

Ozone

The overall 1997–2010 mean of daily maximum eight-hour mean ozone was 73.5 μg m^{-3}. The full-year daily maximum eight-hour ozone concentrations were more evenly distributed among the source regions than those of PM, varying between 69 and 80 μg m^{-3}, with the highest mean at 80 μg m^{-3} associated with air from the northeast. The distribution of observations between the source regions changed as the winter months

Table 1. Summary statistics for hourly observed PM_{10}, $PM_{2.5}$, PN_{UF}, PN_A, BC and daily maximum eight-hour mean surface ozone. Mean, maximum and number of hourly mean concentrations in each sector southwest (SW), southeast (SE), northwest (NW), northeast (NE) and occurrences where the trajectories resided less than 80% of the time in any sector (Multi). The last column shows the mean concentration over all sectors.

	SW	SE	NW	NE	Multi	Mean 1997–2010*
PM_{10}						
Number of hours	16848	5397	7851	6352	45643	
Mean (μg m^{-3})	11.4	22.9	5.7	9.0	10.2	10.8
Max (μg m^{-3})	84.3	123.7	100.7	92.0	103.5	
$PM_{2.5}$						
Number of hours	17679	5281	8151	6816	47348	
Mean (μg m^{-3})	8.5	17.2	4.4	6.7	7.6	8.0
Max (μg m^{-3})	84.9	78.4	65.9	53.8	85.0	
PN_{UF}						
Number of hours	13495	4516	6561	5978	38646	
Mean (cm^{-3}/1000)	1.81	1.32	2.19	1.50	1.68	1.72
Max (cm^{-3}/1000)	31.89	11.10	24.48	10.40	32.72	
PN_A						
Number of hours	13512	4516	6561	5978	38647	
Mean (cm^{-3}/1000)	0.63	1.19	0.26	0.50	0.59	0.59
Max (cm^{-3}/1000)	8.33	5.84	5.44	4.50	9.69	
BC						
Number of hours	8040	2531	4739	4082	25531	
Mean (μg m^{-3})	0.32	0.88	0.13	0.25	0.29	0.32
Max (μg m^{-3})	2.81	5.62	1.67	1.45	5.84	
Mar.–Sep. daily max eight-hour mean ozone						
Number of days	504	133	273	278	1594	
Mean (μg m^{-3})	84	96	76	82	86	85
Max (μg m^{-3})	150	164	108	159	178	
Annual daily max eight-hour mean ozone						
Number of days	919	293	509	423	2544	
Mean (μg m^{-3})	71	75	69	80	75	74
Max (μg m^{-3})	150	164	108	159	178	

* based on years with at least 50% data availability. For overview of data availability *see* Appendix 1.

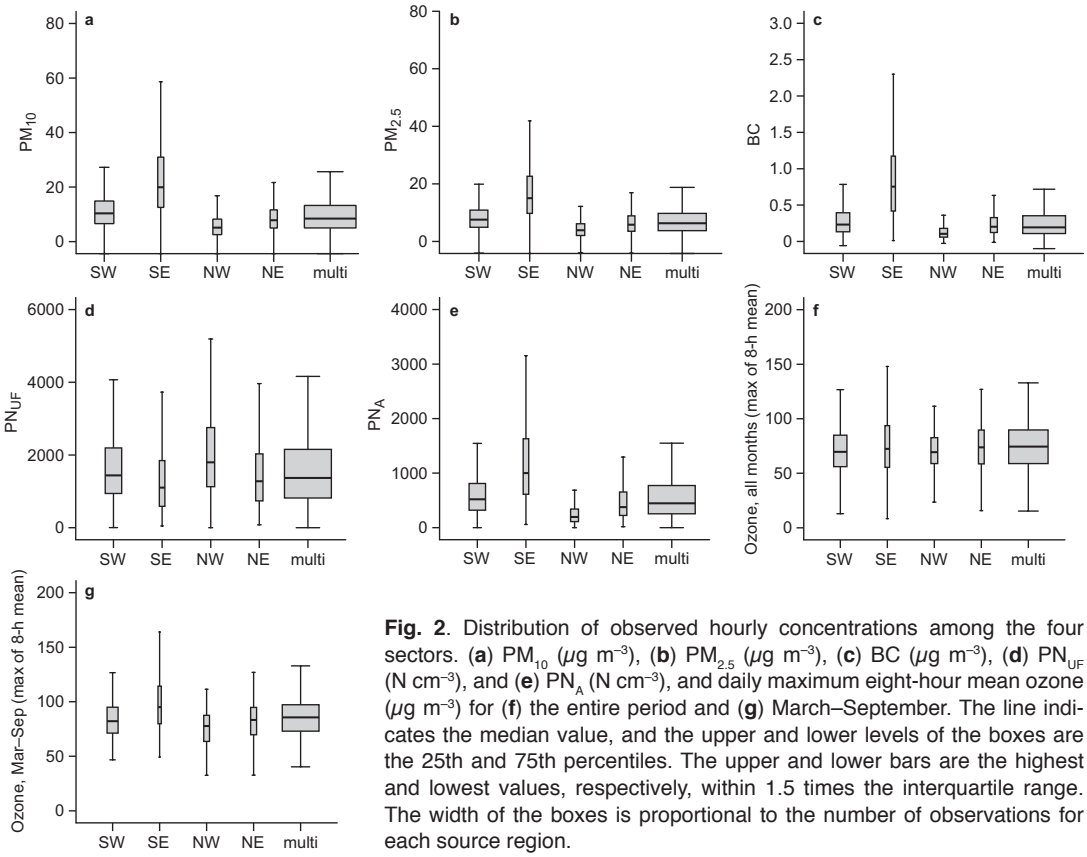

Fig. 2. Distribution of observed hourly concentrations among the four sectors. (**a**) PM_{10} (μg m^{-3}), (**b**) $PM_{2.5}$ (μg m^{-3}), (**c**) BC (μg m^{-3}), (**d**) PN_{UF} (N cm^{-3}), and (**e**) PN_A (N cm^{-3}), and daily maximum eight-hour mean ozone (μg m^{-3}) for (**f**) the entire period and (**g**) March–September. The line indicates the median value, and the upper and lower levels of the boxes are the 25th and 75th percentiles. The upper and lower bars are the highest and lowest values, respectively, within 1.5 times the interquartile range. The width of the boxes is proportional to the number of observations for each source region.

were removed. When this was done, the increase in mean was particularly large (28%) in air from the southeast. Generally, this is due to lower concentrations with weaker gradient across Europe in winter, due to less solar radiation and lower biogenic emissions of ozone precursors. For the period March–September, air from the southeast had higher mean concentration and maximum than air from the other directions.

Air mass origin of the highest concentrations

The highest ~10% daily mean PM_{10}, $PM_{2.5}$ and PN_A concentrations in the measured period occurred when the air originated from the southeast (Fig. 3). The highest daily mean BC concentrations also originated mostly from the south but with a wider spread from the southwest to the east (Fig. 3). For ozone, the high concentration trajectories were even more dispersed, with a source tendency towards the south and east in both high and low altitude trajectories (Fig. 3). However, the tendency was much more pronounced in the southeast direction for the low altitude trajectories. Only about 20% of the trajectories associated with the highest 10% ozone concentrations reached altitudes higher than 2000 m. This means that the highest 10% of the surface ozone concentrations were mainly caused by emissions in Europe (> 80% of the cases) and the stratospheric or non-European contribution was not as important. For the highest PN_{UF}, the air originated from the northwest (Fig. 3), contrary to the origin of the other pollutants.

The geographic distribution of all trajectories reaching Aspvreten during the period 1997–2010 (Fig. 1b) agrees well with the more common westerly and southwesterly wind directions in the area (Alexandersson 2006). The transport patterns of the highest concentrations, except

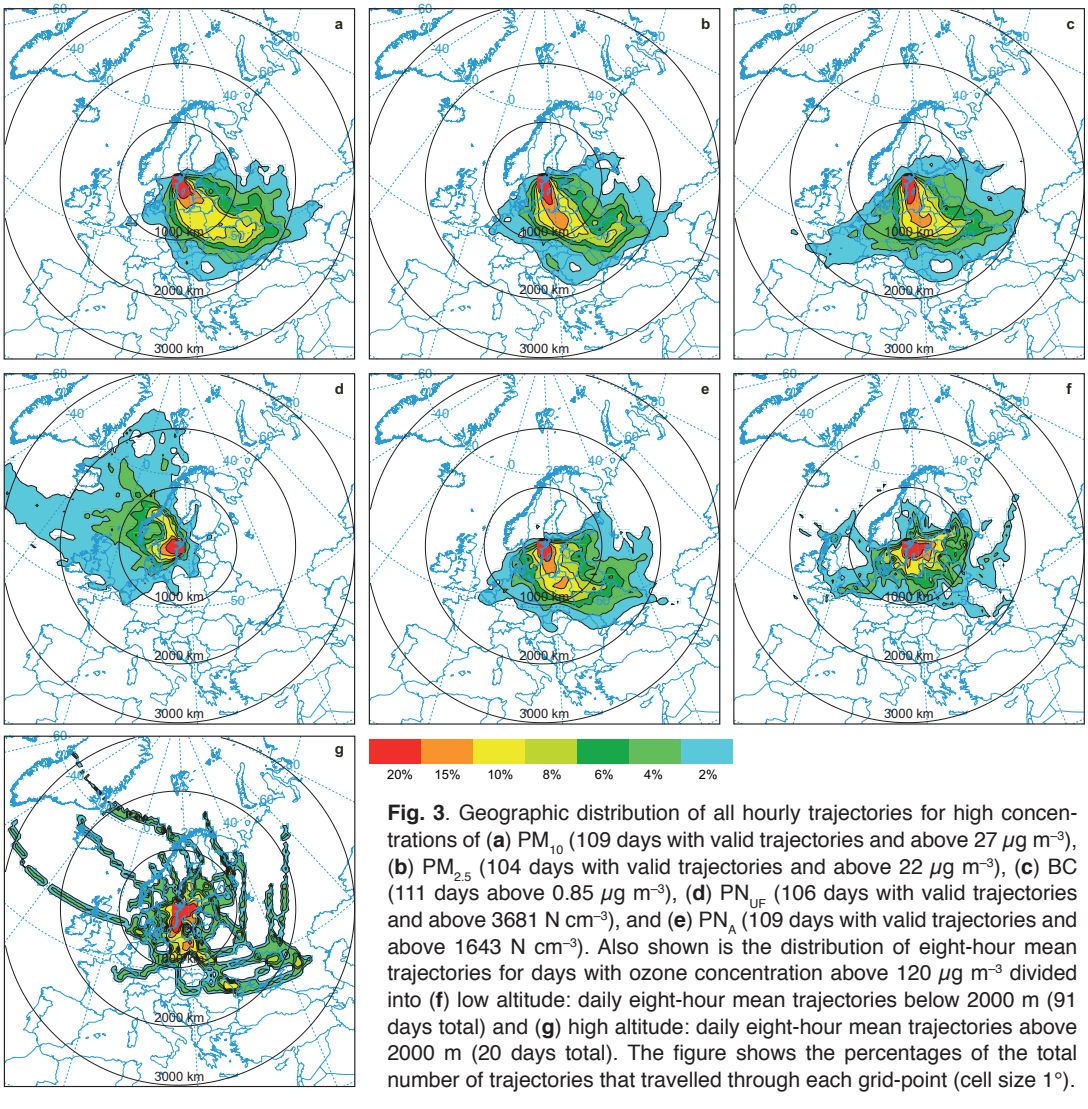

Fig. 3. Geographic distribution of all hourly trajectories for high concentrations of (**a**) PM_{10} (109 days with valid trajectories and above 27 μg m^{-3}), (**b**) $PM_{2.5}$ (104 days with valid trajectories and above 22 μg m^{-3}), (**c**) BC (111 days above 0.85 μg m^{-3}), (**d**) PN_{UF} (106 days with valid trajectories and above 3681 N cm^{-3}), and (**e**) PN_A (109 days with valid trajectories and above 1643 N cm^{-3}). Also shown is the distribution of eight-hour mean trajectories for days with ozone concentration above 120 μg m^{-3} divided into (**f**) low altitude: daily eight-hour mean trajectories below 2000 m (91 days total) and (**g**) high altitude: daily eight-hour mean trajectories above 2000 m (20 days total). The figure shows the percentages of the total number of trajectories that travelled through each grid-point (cell size 1°).

for PN_{UF}, deviated greatly from this pattern. For PN_{UF} the origin of the highest concentrations was shifted slightly towards the northwest.

We also investigated the origins of the very highest observed pollution concentrations. For each pollution episode we included the day of the highest measured pollution (based on diurnal mean for particles and daily max of eight-hour mean for ozone) (*see* Fig. 4). For PM_{10} and ozone, we excluded from the analysis a very strong pollution episode during 30 April–13 May 2006. We discuss this period in more detail below. The trajectories of PM_{10}, $PM_{2.5}$, PN_A and BC further support the conclusion that before reaching Aspvreten, the air containing the very highest concentration originated from the southeast. Out of the five highest daily maximum eight-hour mean ozone concentrations, four originated from the southeast and one from the southwest. The air-mass backward trajectories did not reach as far away for ozone as for the other pollutants. One of the daily maxima originating from the southeast, originated from an altitude higher than 2000 m, but it could not be determined if the reason for the high concentration is transport of ozone-rich air from higher altitudes or from emissions in the trajectory closer to Aspvreten. Finally, the trajectories also

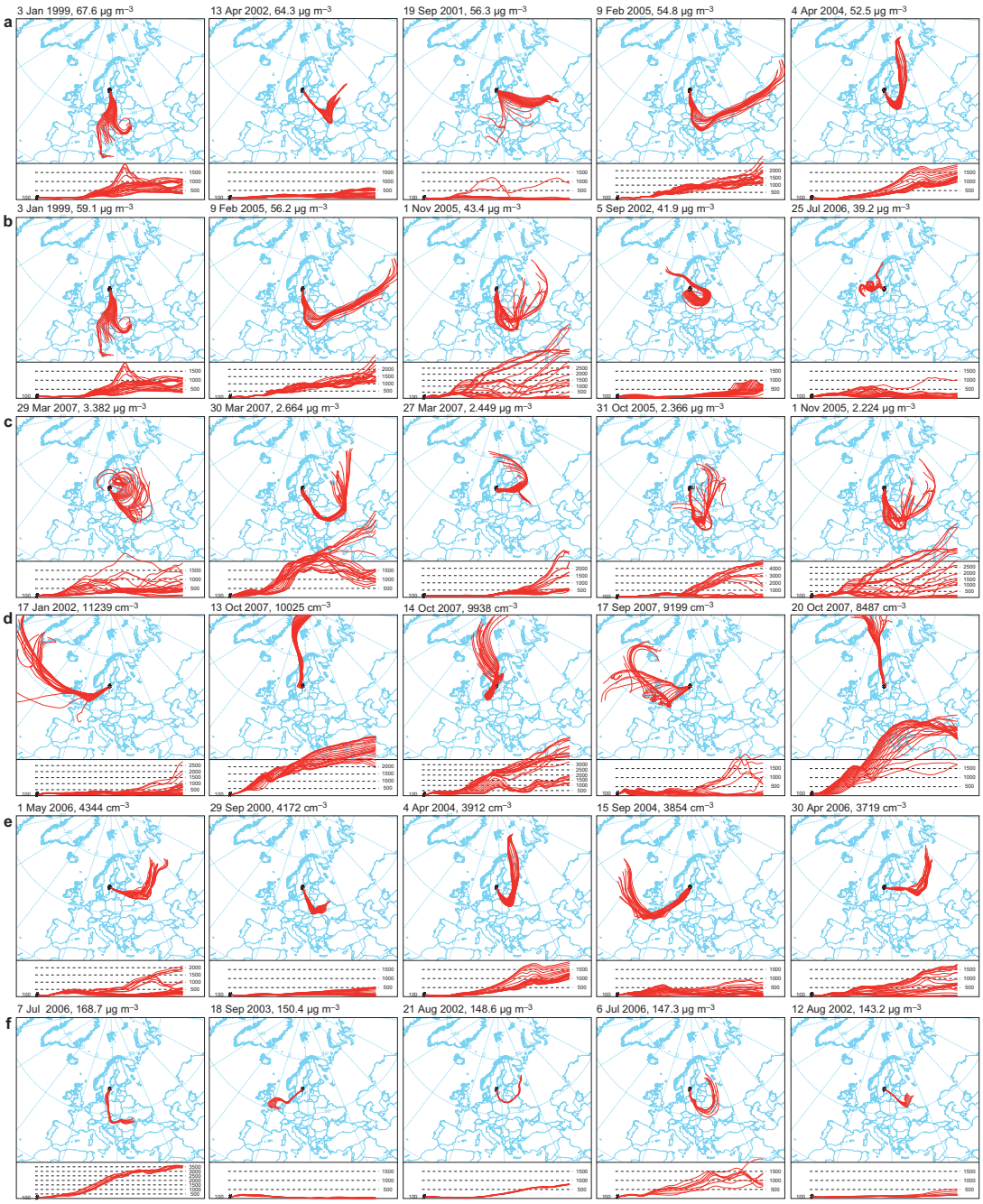

Fig. 4. Hourly air-mass backward trajectories for a selection (*see* text) of the highest observed daily concentrations during 1997–2010: (**a**) PM_{10}, (**b**) $PM_{2.5}$, (**c**) PN_{UF}, (**d**) PN_{A}, (**e**) BC, and (**f**) daily maximum eight-hour mean ozone. Figures are ordered from the highest to the lowest observed level. For PM_{10}, $PM_{2.5}$ and ozone multiple days during the same episode are excluded.

support the conclusion that PN_{UF} was associated with a completely different origin than the other pollutants.

One of the most prolonged ozone episodes, including the highest observed ozone concentrations during the years 1997–2010 in Aspvreten,

lasted from 30 April to 13 May 2006, with 12 days of ozone levels exceeding the target values (Appendix 3). The concentrations on 6 May even exceeded the 180 μg m^{-3} information threshold for the hourly mean. In the beginning of the period, the air originated from east and southeast whereas the air in the second part of the period was circulating slowly above Scandinavia indicating a high pressure event (Appendix 3). During the first days of the episode, the PM_{10} and PN_A concentrations were also unusually high. Further, the PN_{UF} concentrations were unusually high during the episode. The high PM and ozone concentrations indicated transport of polluted air from the east and southeast in the beginning of the period, and a change in weather situation to clear skies and little wind, promoting further ozone formation, while PM_{10} and PN_A dry deposited from the air masses.

Estimated impact on human mortality and source region

We calculated the increase in human mortality relative to the source region that had the lowest concentration, which was the northwest for both $PM_{2.5}$ and ozone. Air masses arriving from the southeast had the highest mean concentrations of air pollution, which resulted in higher risks of premature mortality upon exposure as compared with that caused by exposure to air coming from all other source regions (Table 2). Mortality due to $PM_{2.5}$ exposure would have increased by 7.8%, had the air always come from the southeast not from northwest, i.e. the area with the lowest $PM_{2.5}$ concentration. As compared with air from the northwest, the second highest risk was associated with air from the southwest, with a 3% increase in mortality, followed by the multisector with a 2.4% and northeast with a 1.8% increase in mortality.

In order to estimate the increase in mortality due to the annual mean exposure, we needed to consider the fraction of the total time when air comes from particular sectors. The most common air-mass origin is associated with the southwestern sector. Using the concentrations in the northwest as a baseline causing no increased mortality, air transported from the southwest, southeast, northeast and multisector was estimated to increase premature mortality due to $PM_{2.5}$ exposures by 0.6%, 0.5%, 0.2% and 1.2%, respectively.

As compared with air from the northwest, air masses arriving from the southeast, increased human mortality risk due to ozone exposure on average by 0.6%, this was followed by the multisector with a 0.30% increase, the southwest with a 0.22% increase and the northeast with a 0.18%

Table 2. Contribution of each source sector to premature mortality, due to mean $PM_{2.5}$ and daily maximum eight-hour mean ozone. Shown are the overall mean concentrations in the sectors, proportion of time with air originating from each sector, increased risk of mortality due to elevated concentrations compared to the northwestern sector (NW) and increased risk of mortality weighted by the proportion of time the air originates from each sector (actual risk). We used the data from March–September during the period 1997–2009 for ozone, and all the data in the period 1998–2010 for $PM_{2.5}$.

Measure	SW	SE	NW	NE	Multi
$PM_{2.5}$					
Annual mean (μg m^{-3})	8.5	17.4	4.4	6.7	7.6
Proportion of time (%)	21	6	14	9	51
Increased mortality (%)	3.0	7.8	–	1.8	2.4
Time-weighted increased mortality (%)[a]	0.6	0.5	–	0.2	1.2
Ozone (Mar–Sep)					
Mean (μg m^{-3})[b]	84	96	76	82	86
Proportion of time (%)	18	5	10	10	57
Increased mortality (%)	0.22	0.60	–	0.18	0.30
Time-weighted increased mortality (%)[a]	0.04	0.03	–	0.02	0.17

[a] Weighted by the proportion of time with air is coming from each sector. [b] Based on daily maximum eight-hour mean ozone concentration.

increase. The highest overall increase in mortality (considering the fraction of time air is coming from the sector) was associated with the multi-region with 0.17%, followed by the southwest (0.04%), the southeast (0.03%) and the northeast (0.02%).

Discussion

Seasonal variations in source contributions

As compared with air originating from any other sector, air originating from the southeast had 2–4 times higher concentrations of particulate mass (PM_{10}, $PM_{2.5}$), dominated by accumulation mode particles. We attribute this to emissions in the southeastern sector, i.e. air masses that travelled over pollution sources in continental Europe. Further, the highest 111 daily mean concentrations of PM_{10}, $PM_{2.5}$, PN_A and BC were strongly associated with transport from southeastern Europe, the plotted average origin of these days (*see* Fig. 3) differed significantly from the mean origin of air in Aspvreten (*see* Fig. 1). The highest PM_{10}, $PM_{2.5}$, PN_A and BC concentration days in the highest episodes (*see* Fig. 4 and Appendix 3) were also related to air coming mostly from the southerly and easterly source regions. Most of the trajectories during these days arrived to Aspvreten from the southeast, without passing over areas in Sweden, were local emissions could contribute to the concentrations; hence, these high concentration days were due to the contribution of long-range transport of air pollutants. Some contribution from shipping emissions in the Baltic Sea for air masses classified to the southeastern sector could not be ruled out.

Anthropogenic emissions of air pollution are much higher in continental Europe than in Scandinavia (EMEP 2011a), where natural biogenic VOC emissions are relatively more important for forming secondary organic aerosol (Bergström *et al*. 2012). Some more insight into the importance of anthropogenic *versus* natural sources and primary *versus* secondary particles may be gained by looking at the seasonal variations in the contributions from different sectors (Figs. 5 and 6). Especially for air originating from the southeast, the concentrations are the highest around spring and autumn, except for surface ozone (peak in early summer) and $PM_{2.5}$ (also high during parts of the summer). The increase around spring and autumn may be at least partly related to more frequent long-range transport of particles from agricultural and forest fires in spring and autumn.

By using satellite information in combination with trajectory modelling, Barnaba *et al*. (2011) concluded that the impact of wildfires on Scandinavian aerosol optical thickness has its maximum in April but with a secondary peak also in August. This bimodality is also a known characteristic in agricultural fire activity in eastern Europe and Asian Russia, corresponding to the planting and harvesting periods (Korontzi *et al*. 2006). In Tartu, Estonia, 40% of $PM_{2.5}$ originate from biomass burning sources, whereas 24% originate from industrial processes (Orru *et al*. 2010), further indicating the importance of biomass burning as a source of air pollution in eastern Europe. Hyvärinen *et al*. (2011) found that the highest BC concentrations at five background stations in Finland are associated with long-range transport of anthropogenic pollution from central or eastern Europe, or with agricultural or forest fires, mainly located in eastern Europe. Similar seasonal behaviour of BC concentrations was reported by Byčenkienė *et al*. (2011) for a background site in Lithuania, and they also attribute the increased concentrations in spring and winter to biomass burning and spring wildfires. Differences in meteorological conditions may also be important for the difference between winter and summer, such as more stable conditions (less dilution) during winter increasing the impact of locally emitted air pollution.

For most months, air originating from the southeast had the highest median concentrations of $PM_{2.5}$, PM_{10} and PN_A. Depending on the month, the monthly median BC concentrations were 3–11 times higher in the southeastern sector as compared with those in the northwestern sector. The southeastern sector was particularly important for the median BC concentration; relative to the northwestern sector, BC concentrations were more elevated in the southeastern sector as compared with the contribution of the southeast to PM_{10} and $PM_{2.5}$.

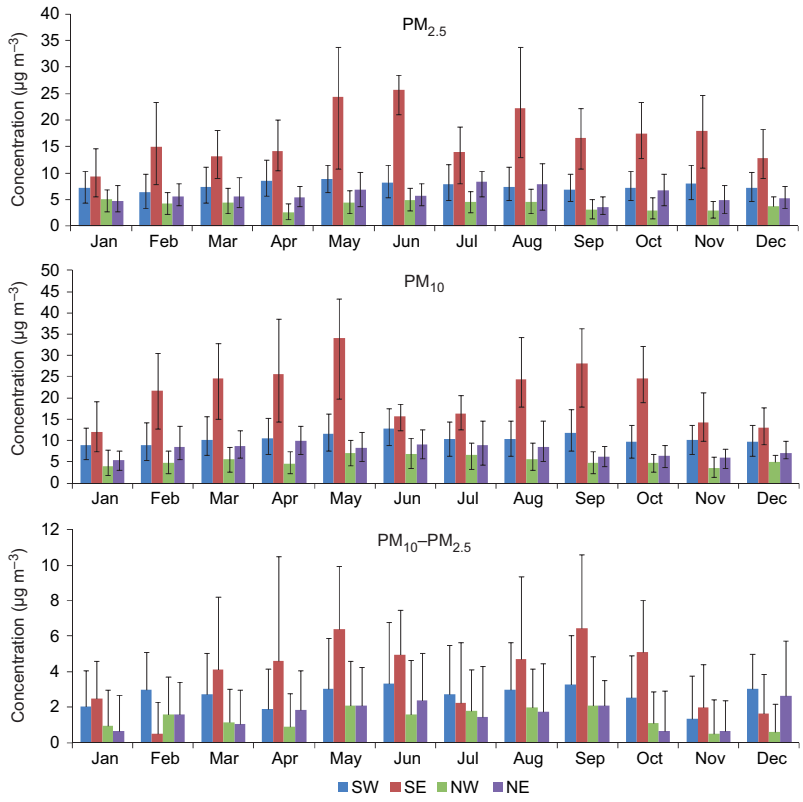

Fig. 5. Monthly median concentrations of $PM_{2.5}$, PM_{10} and PM_{10}–$PM_{2.5}$ (coarse mode particulate matter) concentrations in the four sectors averaged over all available data in the period 1997–2010. Vertical bars are 75 and 25 percentiles.

BC is due to primary anthropogenic emissions (combustion of carbonaceous fuels), as opposed to PM_{10} and $PM_{2.5}$, which are also influenced by secondary particle formation due to both anthropogenic and natural sources as well as contributions from primary natural emissions such as sea salt and suspended dust. Sources of BC peak in winter due to more combustion of carbonaceous fuels, whereas for $PM_{2.5}$ there are other sources, such as photochemical production of secondary organic and inorganic compounds. These make additional contributions to the concentrations in spring and summer (e.g. Putaud *et al*. 2003). This is consistent with the BC-to-$PM_{2.5}$ concentration ratio being higher in winter as compared with that in summer (on average 57 milligrams of BC per a gram of $PM_{2.5}$ for October–March and 29 milligrams of BC per a gram of $PM_{2.5}$ for April–September). This difference in source contributions of BC and $PM_{2.5}$ was particularly pronounced in the southeastern sector, with relatively high primary PM and BC emissions as compared with those in western Europe (Kupiainen and Klimont 2004, EMEP 2010). For coarse particles (PM_{10}–$PM_{2.5}$), there was large variability, but a clear tendency was found towards slightly higher concentrations in air originating from the southeast as compared with those in air originating from the other sectors during spring and autumn.

In contrast to particle mass and accumulation mode particle number concentrations, ultrafine particle number concentrations were typically highest in air originating from the northwest. This finding may be explained by the sources and processes controlling the concentrations of ultrafine particles. In addition to primary ultrafine particles due to combustion processes, nano-sized secondary particles are formed from sulphurous acid and possibly organics (of anthropogenic or biogenic origin) during air mass transport over boreal forest areas mainly in the northerly sectors (Tunved *et al*. 2006). It is well known that formation of new nucleation mode particles from precursor gases depends on the concentration of larger particles that serve as sink for condensable

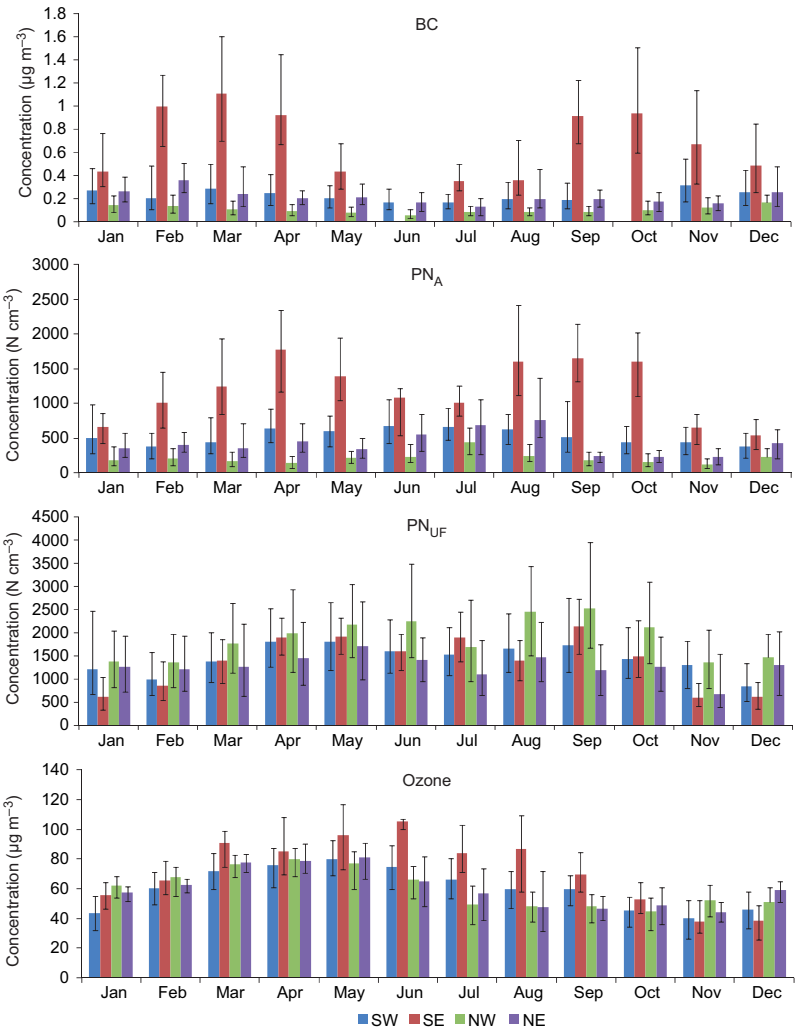

Fig. 6. Monthly median concentrations of BC, PN_A (accumulation mode number concentration), PN_{UF} (ultrafine mode particle number concentration) and daily maximum eight-hour mean ozone concentrations in the four sectors averaged over all available data in the period 1997–2010. Vertical bars are 75 and 25 percentiles.

gases disfavouring nucleation. It has earlier been found that nucleation is largely absent, and that number concentrations decrease as air is transported from the south over Scandinavia (Tunved *et al*. 2005). When air is of continental European origin, primary emission is a more important source of ultrafine particle number concentrations than nucleation (Tunved *et al*. 2010). Lowest concentrations are seen during the winter, indicating the importance of secondary particle formation as compared with that of primary particle emissions. But even during winter, air masses from the north have higher number concentrations as compared with air from the south which could be related to the higher concentrations of accumulation mode particles in southern air masses, promoting coagulation of nucleation mode particles with larger particles as noted in calculations by Tunved *et al*. (2010).

For ozone, the differences between source region averages for the whole period were small based on the full year of data. For the summer period (March–September), air originating from the southeast had higher mean concentrations than the other source regions. In fact, the southeast contributed higher median concentration for all the months from March to October (*see* Fig. 6). However, ozone concentrations show less distinct source-based pattern than what was seen for the PM concentrations. This is probably due to ozone being more dependent on meteorological condition and due to more complex

chemistry than that of some of the particle components (e.g. primary particles). Most favorable meteorological condition for ozone production is calm, dry and sunny weather, often encountered in high-pressure weather systems (Tang *et al*. 2009a). This is coupled to increasing temperature and clear weather promoting primary biogenic emissions and peroxy-acetyl nitrate decomposition. Nonetheless, the origin of the highest ozone concentrations was predominantly southerly and easterly. The southeastern sector is of less importance for ozone than for PM.

There was a wider geographic spread among the highest 10% ozone back trajectories that reached above 2000 m than among those closer to the ground. A lower trajectory altitude throughout the back trajectory is likely to give a stronger signal of important emission sources, and the back trajectories below 2000 m do indicate the south and the east as more important source regions. Further, the trajectories for the five highest surface ozone concentration days (> 143.2 μg m^{-3}) were mostly travelling from the south of Aspvreten. Finally, the trajectories with the highest ozone concentrations were notably shorter than the trajectories with the highest particle concentrations. The slow-moving air trajectories further support the conclusion that stagnant weather conditions are largely responsible for the highest ozone concentrations. This study presents a further proof that days with high ozone concentrations in regional background in Sweden are mainly related to anti-cyclonic weather events and air originating from southeast/east and southwest/south, which was also found by Tang *et al*. (2009b).

In the beginning of the episode April/May 2006, both PM_{10} and ozone concentrations were constantly elevated, likely because of windy conditions that caused downward mixing of ozone from within the atmospheric boundary layer to replace close-ground ozone as it was degraded (deposited) during night. Trajectories during the first days were also to a large extent close to the surface over eastern Europe. This together with the high PM_{10} concentrations show that transport from eastern Europe was associated with the high concentrations in the early part of the episode. Many of the trajectories started at higher altitudes, so it could not be excluded that downward transported ozone also contributed. Later in the episode the PM_{10} concentration decreased while the ozone concentrations were still elevated. The diurnal ozone pattern was also more pronounced, with deeper nighttime reductions of the concentrations. This indicates that clear skies promote ozone formation during day and depletion close to the surface during night.

The location of Aspvreten close to the Baltic Sea may be partly responsible for maintaining higher ozone concentrations in air from the southeast than from the other regions, as the dry deposition of ozone is less effective over water than over vegetated areas (e.g. Erisman *et al*. 1994). Air originating from southeastern Europe travels over the Baltic Sea; hence this would act to conserve the ozone as compared with when the air is moving over land. This means that emissions in southeastern Europe might contribute more than those in other regions to high ozone concentrations in Aspvreten merely due to the geographic circumstances.

Table 3. Aggregated emissions (Tg yr^{-1}) described by EMEP (http://www.ceip.at) for 2001 and 2008, aggregated over EEU and WEU. *See* Fig. 1 for explanation of countries belonging to EEU and WEU.

	WEU		EEU	
	2001	2008	2001	2008
NO_x	9.5	7.4	8.0	9.6
NMVOC	8.3	6.0	7.2	7.9
$PPM_{2.5}$	1.1	0.9	2.0	1.9
SO_x	5.2	2.5	13.0	10.9
CO	27.8	19.0	31.3	32.2

Concentrations in relation to emissions in eastern and western Europe

We aggregated EMEP emissions (http://www.ceip.at) over southeastern and southwestern Europe for the years 2001 and 2008 (Table 3). The EMEP emissions are reported by nations and regions, and the geographical heterogeneity of emissions within each area can be large. The actual emissions along the trajectories can therefore be very different than for the entire region and these results should only be used as an

indication of the actual emissions in the regions. Nonetheless, the reported EMEP emissions suggest that eastern Europe (EEU, *see* Fig. 1) is responsible for higher emissions of primary PM ($PPM_{2.5}$), which are about twice as high as those of western Europe (WEU, *see* Fig. 1). This is qualitatively consistent with the results from this study: air from the southeast had nearly twice as high mean concentrations of both PM_{10} and $PM_{2.5}$ as those in air of the southwest origin. However, it is not only primary PM that contributes to the PM concentration, but also the emissions of gases such as SO_x, NO_x, NH_3 and NMVOCs (both anthropogenic and biogenic) forming PM in the atmosphere. According to the EMEP emission inventory for the two years, SO_x emissions are also greater in eastern than in western Europe. The region of largest emissions of NO_x and NMVOC, which are ozone and particle precursors, changed within the study period: in 2001, the emissions of NO_x and NMVOCs were about 15% and 19% higher, respectively, in western than in eastern Europe, but in 2008 those emissions were 30% and 32% higher, respectively, in eastern than in western Europe. The change is due to both increasing emissions in the east and decreasing emissions in the west. The relative contribution to ozone concentrations by the two regions (southeast and southwest), estimated by us, falls somewhere in-between the two years of the EMEP data; hence the contributions to the mean concentration can be explained by differences in anthropogenic emissions reported to EMEP. However the geographical differences in the EMEP emission data do not explain why the east contributes in such a large degree to the very highest observed concentrations. These episodes are probably due to emissions not reported to EMEP, such as agricultural or forest fires. For example, the episode in spring 2006 has been shown to be due to the uncontrolled burning of agricultural crop residues in Belarus, Baltic countries, Ukraine and western Russia and the influence on a number of pollutants was detected in the Arctic (Stohl *et al*. 2007, Treffeisen *et al*. 2007), northern Europe (Saarikoski *et al*. 2007, Sopauskiene and Jasineviciene 2009) and the United Kingdom (Witham and Manning 2007). Deficiencies in the EMEP emission inventory are not limited to non-reported fires, but may also include biases, both positive and negative, that can be region specific.

Based on the trajectory modelling made in this study, we cannot assess the influence of emissions from the Baltic Sea traffic. Such emissions would contribute to PM_{10}, $PM_{2.5}$ and BC for the southeast source region. As these sea emissions add to the source–receptor relationship with eastern Europe, it would be beneficial to investigate their contributions to the values measured in Aspvreten.

During the last four years (2006–2010), in all sectors there was a tendency of decreasing annual median concentrations of especially $PM_{2.5}$ and PM_{10} (Fig. 7). Looking at the southeastern sector, this tendency is evident also for BC and PN_A (Fig. 8). These observations are in qualitative agreement with the trends in emissions of $PM_{2.5}$ and its precursor gases as reported by EMEP (EMEP 2011a), but — as expected from the emission inventory — the concentrations in the period 1997–2005 were not systematically higher than those in 2006. It should be noted that the annual median concentrations are not only dependent on emissions but are also affected by differences in meteorological conditions. For the median of the maximum eight-hour mean ozone and PN_{UF} there is no systematic trend in any sector (Fig. 8).

Impact of source region on population mortality

Air mass transport from the southeast of Aspvreten is relatively more important for the increased risk of human mortality. This implies that if in future Sweden were to experience southeastern winds more often, health effects of the Swedish population would be greater (if emissions remain the same in Europe). Efforts to decrease emissions in eastern Europe would reduce the risks and associated deaths in Sweden, but also locally in eastern Europe as well as in other areas downwind from that region. The increased risks were estimated using mean source region concentrations without considering that there are large variations of the daily concentrations for the days assigned to each source region. However, this is justified as

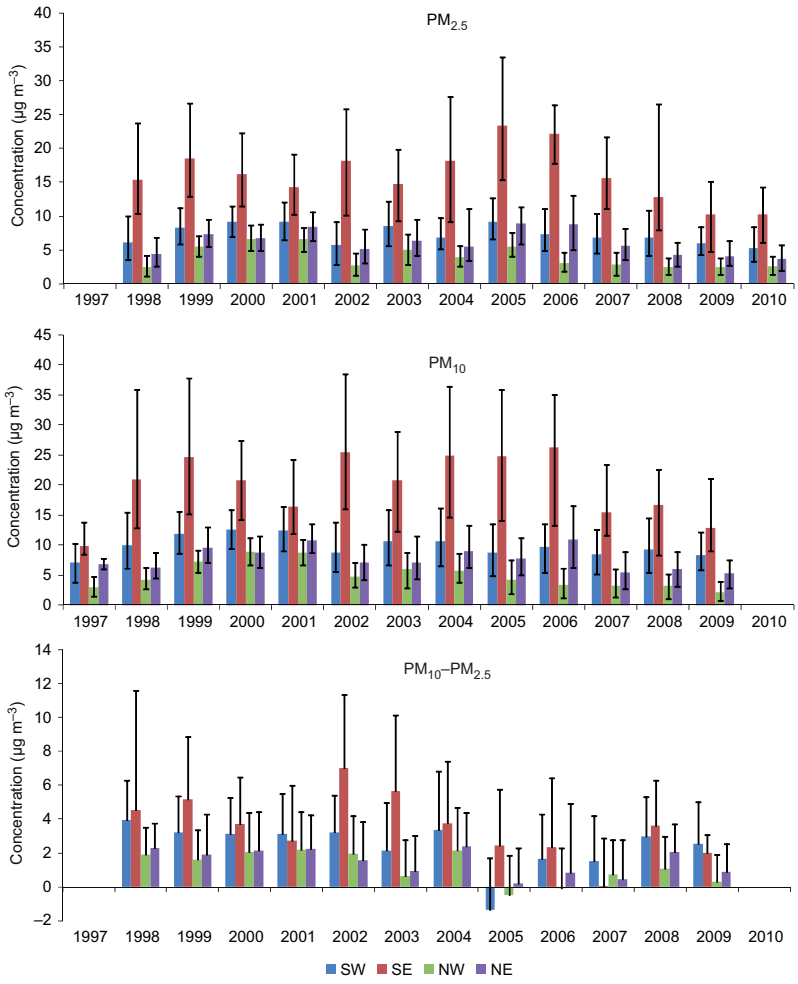

Fig. 7. Annual median concentrations of $PM_{2.5}$, PM_{10} and PM_{10}–$PM_{2.5}$ concentrations in the four sectors. Vertical bars are 75 and 25 percentiles.

long as the dose-response function is independent of the concentrations.

It should be kept in mind that the increased mortality risk due to $PM_{2.5}$ exposure is based on a dose-response coefficient from long-term exposure epidemiological studies (Ballester *et al*. 2008). The division of exposures into contributions from different source regions splits the period into many short-term exposures lasting for a few days. This exposure variability may not have the same health effect as presented in the epidemiological studies. There are also many other factors that contribute to the uncertainty, e.g. potentially different health effects due to different chemical composition and synergistic effects among pollutants that could be systematically different among the source regions. In a study of PM toxicity, which was indicated by oxidative properties of $PM_{2.5}$, in Tartu, it was found that air masses from Russia and eastern Europe had approximately 1.5 times higher oxidative capacity (Orru *et al*. 2010).

Conclusions

We categorised observed rural background concentrations of aerosol and surface ozone in Sweden based on air-mass origin using hourly air-mass backward trajectories during 14 years. This method is independent of uncertainties related to emissions and atmospheric transformation, hence the results can be used in an independent evaluation of model or emission data. We draw the following conclusions from this work:

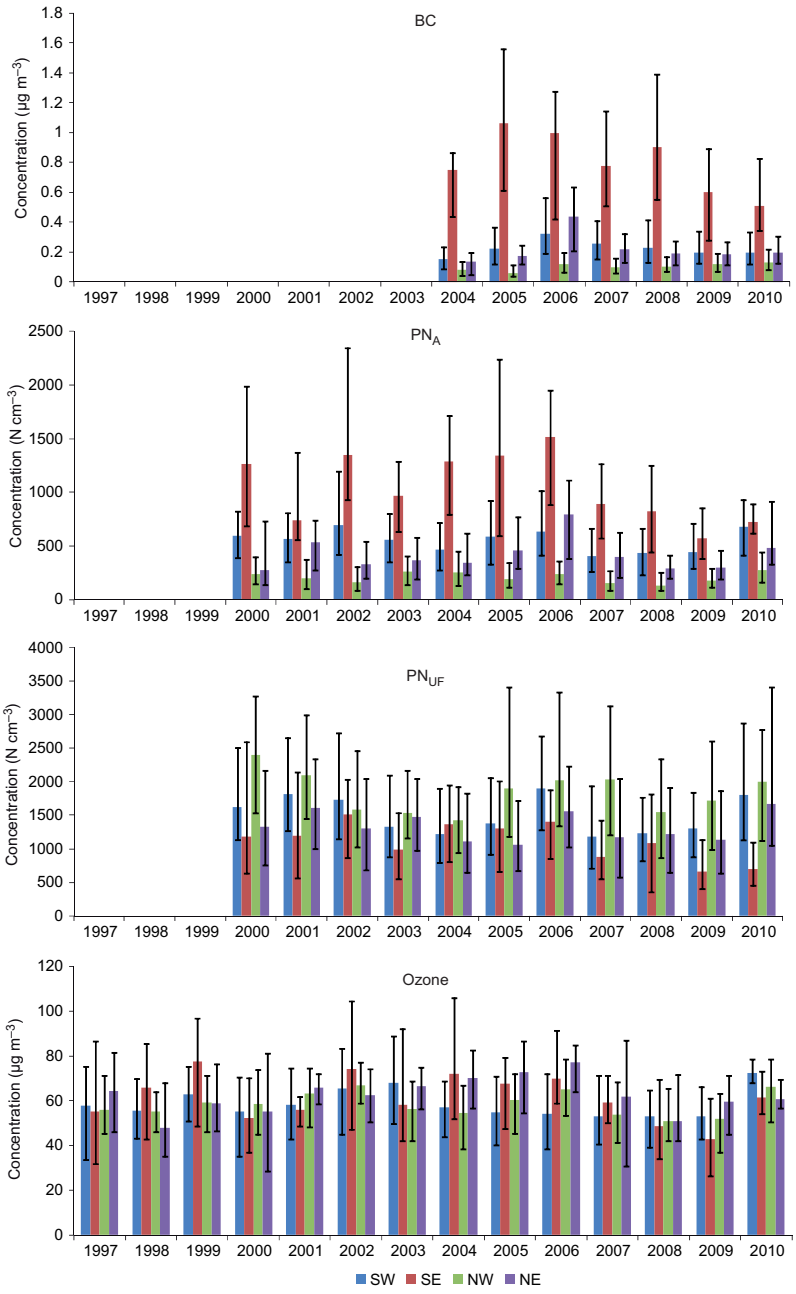

Fig. 8. Annual median concentrations of BC, PN_A (accumulation mode number concentration), PN_{UF} (ultrafine mode particle number concentration) and daily maximum eight-hour mean ozone concentrations in the four sectors. Vertical bars are 75 and 25 percentiles.

— The highest concentrations of $PM_{2.5}$, PM_{10}, BC, number of accumulation mode particles as well as daily eight-hour maximum surface ozone were associated with air masses arriving from eastern Europe. In the southeastern European air masses, the mean values of $PM_{2.5}$, PM_{10}, PN_A, BC and ozone were 3.9, 4.0, 6.8, 4.6, and 1.3 times higher, respectively, as compared with air masses from northwest.

— For the particle components, except ultrafine particle number, the southeast contributes higher concentrations than the other sectors. This is consistent for all years. The sector contributing highest concentrations to surface ozone varied between the years.

— The largest contribution of PM_{10}, BC and accumulation mode particle number occurred from southeastern Europe in spring and autumn. For $PM_{2.5}$ the contribution from the southeast was also large during summer.
— The accumulation mode particles dominated the mass of $PM_{2.5}$ and PM_{10}.
— The highest ultrafine particle number were associated with clean air masses from the northwest.
— Western continental Europe was also an important contributor to high concentrations of $PM_{2.5}$, PM_{10}, BC and surface ozone in Sweden as compared with concentrations from the northern sectors. Since air masses originating from the west were more common than air from the east, air masses from the southwest affected health more negatively than air masses from the southeast. Therefore, efforts to improve Swedish background air quality should be taken to reduce emissions in both eastern and western Europe, but in order to reduce the very highest concentrations emissions in the eastern Europe must be targeted.
— For PM and BC, the findings are in agreement with the EMEP emission data for eastern and western Europe, which — in line with the results of this study — indicate that eastern Europe is more responsible for emissions of primary PM and SO_2 than western Europe.

Acknowledgements: This work was supported by the Swedish Clean Air Research Programme (SCARP). We thank Dr. Peter Tunved for his expert advice on running and analyzing trajectories.

References

Abdalmogith S.S. & Harrison R.M. 2005. The use of trajectory cluster analysis to examine the long-range transport of secondary inorganic aerosol in the UK. *Atmos. Environ.* 39: 6686–6695.

Alexandersson H. 2006. *Vindstatistik för Sverige, 1961–2004*. SMHI report Meteorologi nr 121, Swedish Meteorological and Hydrological Institute, Norrköping.

Andersson C., Bergström R. & Johansson C. 2009. Population exposure and mortality due to regional background PM in Europe — long-term simulations of source region and shipping contributions. *Atmos. Environ.* 43: 3614–3620.

Areskoug H., Camner P., Dahlen S.-E., Låstbom L., Nyberg F., Pershagen G. & Sydbom A. 2000. Particles in ambient air — a health risk assessment. *Scand. J Work Environ. Health* 26, Supplement 1: 1–96.

Ballester F., Medina S., Boldo E., Goodman P., Neuberger M., Iñiguez C. & Künzli N. 2008. Reducing ambient levels of fine particles could substantially improve health: a mortality impact assessment for 26 European cities. *J. Epidemiol. Community Health* 62: 98–105.

Barnaba F., Angelini F., Curci G. & Gobbi G.P. 2011. An important fingerprint of wildfires on the European aerosol load. *Atmos. Chem. Phys.* 11: 10487–10501.

Bergström R., Denier van der Gon H.A.C., Prévôt A.S.H., Yttri K.E. & Simpson D. 2012. Modelling of organic aerosols over Europe (2002–2007) using a volatility basis set (VBS) framework with application of different assumptions regarding the formation of secondary organic aerosol. *Atmos. Chem. Phys.* 12: 8499–8527.

Byčenkienė S., Ulevicius V. & Kecorius S. 2011. Characteristics of black carbon aerosol mass concentration over the East Baltic region from two-year measurements. *J. Environ. Monit.* 13: 1027–1038.

Draxler R.R. & Hess G.D. 1998. An overview of the HYSPLIT_4 modelling system for trajectories, dispersion and deposition. *Australian Meteorological Magazine* 47: 295–308.

Dvorská A., Lammel G. & Holoubek I. 2009. Recent trends of persistent organic pollutants in air in central Europe — air monitoring in combination with air mass trajectory statistics as a tool to study the effectivity of regional chemical policy. *Atmos. Environ.* 43: 1280–1287.

Eliassen A. 1978. The OECD study of long range transport of air pollutants: long range transport modelling. *Atmos. Environ.* 12: 479–487.

EMEP 2010. *Transboundary particulate matter in Europe*. Status report 4/2010, O98134, Norwegian Chemical Co-ordinating Centre of EMEP, Norwegian Institute for Air Research, Kjeller.

EMEP 2011a. *Transboundary acidification, eutrophication and ground level ozone in Europe in 2009*. Status report 1/2011, Norwegian Chemical Co-ordinating Centre of EMEP, Norwegian Institute for Air Research, Kjeller.

EMEP 2011b. *Transboundary particulate matter in Europe*. Status report 4/2011, Norwegian Chemical Co-ordinating Centre of EMEP, Norwegian Institute for Air Research, Kjeller.

Erisman J.E., Van Pul A. & Wyers P. 1994. Parametrization of surface resistance for the quantification of atmospheric deposition of acidifying pollutants and ozone. *Atmos. Environ.* 28: 2595–2607.

Fleming Z.L., Monks P.S. & Manning A.J. 2012. Review: Untangling the influence of air-mass history in interpreting observed atmospheric composition. *Atmospheric Research* 104–105: 1–39.

Forsberg B., Hansson H.-C., Johansson C., Areskoug H., Persson K. & Järvholm B. 2005. Comparative health impact assessment of local and regional particulate air pollutants in Scandinavia. *Ambio* 34: 11–19.

Forsström S., Ström J., Pedersen C.A., Isaksson E. & Gerland, S. 2009. Elemental carbon distribution in Svalbard snow. *J. Geophys. Res.* 114, D19112, doi:10.1029/2008JD011480.

Gryparis A., Forsberg B., Katsouyanni K., Analitis A., Tou-

loumi G., Schwartz J., Samoli E., Medina S., Anderson H.R., Niciu E.M., Wichmann H.E., Kriz B., Kosnik M., Skorkovsky J., Vonk J.M. & Dortbudak Z. 2004. Acute effects of ozone on mortality from the "Air pollution and health: a European approach" project. *Am. J. Respir. Crit. Care Med*. 170: 1080–1087.

Hyvärinen A.-P., Kolmonen P., Kerminen V.-M., Virkkula A., Leskinen A., Komppula M., Hatakka J., Burkhart J., Stohl A., Alto P., Kulmala M., Lehtinen K.E.J., Viisanen Y. & Lihavainen H. 2011. Aerosol black carbon at five background measurement sites over Finland, a gateway to the Arctic. *Atmos. Environ*. 45: 4042–4050.

Korontzi S., McCarty J., Loboda T., Kumar S. & Justice C. 2006. Global distribution of agricultural fires in croplands from 3 years of moderate resolution imaging spectroradiometer (MODIS) data. *Global Biogeochem. Cycles* 20, GB2021, doi:10.1029/2005GB002529.

Krecl P., Targino A.C. & Johansson C. 2011. Spatiotemporal distribution of light-absorbing carbon and its relationship to other atmospheric pollutants in Stockholm. *Atmos. Chem. Phys*. 11: 11553–11567.

Krupa S.V. & Manning W.J. 1988. Atmospheric ozone: formation and effects on vegetation. *Environ. Pollut*. 50: 101–137.

Kukkonen J., Olsson T., Schultz D.M., Baklanov A., Klein T., Miranda A.I., Monteiro A., Hirtl M., Tarwainen V., Boy M., Peuch V.-H., Poupkou A., Kioutsioukis I., Finardi S., Sofiev M., Sokhi R., Lehtinen K.E.J., Karatzas K., San José R., Astitha M., Kallos G., Schaap M., Reimer E., Jakobs H. & Eben K. 2012. A review of operational, regional-scale, chemical forecasting models in Europe. *Atmos. Chem. Phys*. 12: 1–87.

Kulmala M., Asmi A., Lappalainen H.K., Carslaw K.S., Pöschl U., Baltensperger U., Hov Ø., Brenquier J.-L., Pandis S.N., Facchini M.C., Hansson H.-C., Wiedensohler A. & O'Dowd C.D. 2009. Introduction: European Integrated Project on Aerosol Cloud Climate and Air Quality interactions (EUCAARI) — integrating aerosol research from nano to global scales. *Atmos. Chem. Phys*. 9: 2825–2841.

Kupiainen K. & Klimont Z. 2004 *Primary emissions of Submicron and carbonaceous particles in Europe and the potential for their control*. IR-04-079, International Institute for Applied Systems Analysis, Laxenburg, Austria.

Lee B.-K., Lee H.K. & Jun N.-Y. 2006. Analysis of regional and temporal characteristics of PM_{10} during an Asian dust episode in Korea. *Chemosphere* 63: 1106–1115.

Lee S. & Ashbaugh L. 2007. The impact of trajectory starting heights on the MURA trajectory source apportionment (TSA) method. *Atmos. Environ* 41: 7022–7036.

Orru H., Kimmel V., Kikas Ü., Soon A., Künzli N., Schins R.P.F., Borm P.J.A. & Forsberg B. 2010. Elemental composition and oxidative properties of $PM_{2.5}$ in Estonia in relation to origin of air masses — results from the ECRHS II in Tartu. *Sci. Total Environ*. 408: 1515–1522.

Philipin S., Laj P., Putaud J.-P., Wiedensohler A., De Leeuw G., Flearra A.M., Platt U., Baltensperger U. & Fiebig M. 2009. EUSAAR — an unprecedented network of aerosol observations in Europe. *Earozoru Kenkyu* 24: 78–83.

Pope C.A.III & Dockery D.W. 2006. Health effects of fine particulate air pollution: Lines that connect. *J Air Waste Manag Assoc*. 56: 709–742.

Pope C.A.III, Burnett R.T., Thun M.J., Calle E.E., Krewski D., Ito K. & Thurston G.D. 2002. Lung cancer, cardiopulmonary mortality, and long-term exposure to fine particulate air pollution. *JAMA* 287: 1137–1141.

Putaud J.-P., Van Dingenen R., Baltensperger U., Brüggemann E., Charron A., Facchini M.C., Decesari S., Fuzzi S., Gehrig R., Hansson H.-C., Harrison R.M., Jones A.M., Laj P., Lorbeer G., Maenhaut W., Mihalopoulos M., Müller K., Palmgren F., Querol X., Rodriguez S., Schneider J., Spindler G., ten Brink H., Tunved P., Tørseth K., Wehner B., Weingartner E., Wiedensohler A., Wåhlin P. & Raes F. 2003. *A European aerosol phenomenology*. Joint Research Centre Institute for Environment and Sustainability, Ispra, Italy, available at http://ccaqu.jrc.ec.europa.eu/Publication/Phenomenology.pdf.

Rodhe H. 1972. A study of the sulfur budget for the atmosphere over northern Europe. *Tellus* 24: 128–138.

Saarikoski S., Sillanpää M., Sofiev M., Timonen H., Saarnio K., Teinilä K., Karppinen A., Kukkonen J. & Hillamo R. 2007. Chemical composition of aerosols during a major biomass burning episode over northern Europe in spring 2006: experimental 656 and modeling assessments. *Atmos. Environ*. 41: 3577–3589.

Sopauskiene D. & Jasineviciene D. 2009. Variations of concentration of aerosol particles (< 10 μm) in Vilnius. *Lith. J. Phys*. 49: 323–334.

Stohl A. 1998. Computation, accuracy and applications of trajectories — a review and bibliography. *Atmos. Environ*. 32: 947–966.

Stohl A., Berg T., Burkhart J.F., Fjæraa A.M., Forster C., Herber A., Hov Ø., Lunder C., McMillan W.W., Oltmans S., Shiobara M., Simpson D., Solberg S., Stebel K., Ström J., Tørseth K., Treffeisen R., Virkkunen K. & Yttri K.E. 2007. Arctic smoke — record high air pollution levels in the European Arctic due to agricultural fires in Eastern Europe in spring 2006. *Atmos. Chem. Phys*. 7: 511–534.

Tang L., Karlsson P.E., Gu Y., Chen D. & Grennfelt P. 2009a. Synoptic weather types and long-range transport patterns for ozone precursors during high-ozone events in southern Sweden. *Ambio* 38: 459–464.

Tang L., Chen D., Karlsson P.-E., Gu Y. & Ou T. 2009b. Synoptic circulation and its influence on spring and summer surface ozone concentrations in southern Sweden. *Boreal Env. Res*. 14: 889–902.

Treffeisen R., Tunved P., Ström J., Herber A., Bareiss J., Helbig A., Stone R.S., Hoyningen-Huene W., Krejci R., Stohl A. & Neuber R. 2007. Arctic smoke-aerosol characteristics during a record smoke event in the European Arctic and its radiative impact. *Atmos. Chem. Phys*. 7: 3035–3053.

Tunved P., Hansson H.-C., Kulmala M., Aalto P., Viisanen Y., Karlsson H., Kristensson A., Swietlicki E., Dal Maso M., Ström J. & Komppula M. 2003. One year boundary layer aerosol size distribution data from five Nordic background stations. *Atmos. Chem. Phys*. 3: 2183–2205.

Tunved P., Nilsson E.D., Hansson H.-C., Ström J., Kulmala M., Aalto P. & Viisanen Y. 2005. Aerosol characteristics

of air masses in northern Europe: influences of location, transport, sinks, and sources. *J. Geophys. Res.* 110, D07201, doi:10.1029/2004JD005085.

Tunved P., Hansson H.-C., Kerminen V.-M., Ström J., Dal Maso M., Lihavainen H., Viisanen Y., Aalto P.P., Komppula M. & Kulmala M. 2006. High natural aerosol loading over boreal forests. *Science* 312: 261–263.

Tunved P., Partridge D.G. & Korhonen H. 2010. New trajectory-driven aerosol and chemical process model Chemical and Aerosol Lagrangian Model (CALM). *Atmos. Chem. Phys.* 10: 10161–10185.

Witham C. & Manning A. 2007. Impacts of Russian biomass burning on UK air quality. *Atmos. Environ.* 41: 8075–8090.

WHO 2006. *Air quality guideline, global update 2005*. World Health Organization Regional Office for Europe, Copenhagen, Denmark.

WHO 2008. *Health risks of ozone from long-range transboundary air pollution*. World Health Organization Regional Office for Europe, Copenhagen, Denmark.

Appendix 1. Hourly measurement-data availability (%) and annual averages (μg m^{-3}) at Aspvreten.

Year	Ozone		PM_{10}		$PM_{2.5}$		BC		PN_{UF}		PN_{A}	
	Availablitity	Average	Availablitity	Average	Availablitity	Average	Availablitity	Average	Availablitity	Average	Availablitity	Average
1997	97	73.8	10	–*	–	–	–	–	–	–	–	–
1998	97	67.8	86	10.2	81	7.0	–	–	–	–	–	–
1999	92	77.4	70	12.8	73	9.5	–	–	–	–	–	–
2000	84	70.7	89	12.7	92	9.6	–	–	50	–	50	–
2001	88	70.7	78	12.6	79	9.5	–	–	62	2077	62	540
2002	95	81.5	76	10.7	76	7.3	–	–	71	1804	71	680
2003	96	78.2	85	10.7	86	8.4	–	–	74	1651	74	544
2004	96	72.4	98	11.4	84	7.5	26	–*	90	1417	90	594
2005	97	73.8	97	10.1	90	10.3	95	0.31	95	1607	95	672
2006	94	83.4	98	10.9	51	8.6	82	0.38	86	2089	86	799
2007	92	71.6	94	8.35	97	7.1	86	0.33	98	1898	98	515
2008	95	68.6	88	8.64	71	7.0	84	0.30	94	1476	94	474
2009	100	65.8	32	–*	91	5.9	91	0.29	94	1421	94	475
2010	47	–*	–	–	70	5.7	88	0.29	25	–	25	–

* We required at least 50% data capture for calculation of annual average.

Appendix 2. Sensitivities in trajectory simulation

We conducted sensitivity tests (Table A2-1) in order to study the robustness of the results due to choices in trajectory modelling settings and input data. We performed a sensitivity test on the two meteorological datasets for the year 2005. In order to estimate the effect of different starting heights, we produced trajectories for starting heights of 100 m (default), 250 m and 700 m above ground level but within the atmospheric boundary layer. We also tested for differences caused by using an alternative starting location ca. 187 km north/north-west (a different starting grid point) of the original position, in order to estimate the influence of the horizontal starting position on the source classification.

The result of the sensitivity analysis of the trajectory modelling shows that the daily average backward trajectories produced for 2005 for the five sensitivity simulations had the same source region classification for 63%–87% of the cases (Table A2-2). The relative number of days originating from the different source regions changed only slightly depending on the daily trajectories produced under the different sensitivity runs (Table A2-3).

The influence on source-region based daily-average PM_{10} and ozone concentrations varied somewhat for the different sensitivity runs (Fig. A2-1). While small, the largest variations in average PM_{10} between the sensitivity runs occurred for the southeastern source region. This is to some extent likely due to the southeast having the lowest number of samples and widest spread in concentrations.

The chosen starting height affected the PM_{10} results to some extent. The largest effect was

Table A2-1. Setup of the sensitivity analysis of daily average back trajectories for 2005.

Simulation	Main	$GDAS_{100}$	FNL_{100}	$GDAS_{250}$	$GDAS_{700}$	$GDAS_{hs}$
Starting height at Aspvreten	100 m	100 m	100 m	250 m	700 m	100 m
Dataset	FNL 1997–2004 GDAS 2005–2010	GDAS	FNL	GDAS	GDAS	GDAS
Position	58.8°N, 17.38°E	58.8°N, 17.38°E	58.8°N, 17.38°E	58.8°N, 17.38°E	58.8°N, 17.38°E	60.3°N, 15.9°E

Table A2-2. Source-region classification agreement for 2005 between different sensitivity runs for daily average trajectories for cases presented in Table B1. The agreement is expressed as a percentage of trajectories that were classed as originating from the same sector by both simulations.

Simulation	FNL_{100}	$GDAS_{250}$	$GDAS_{700}$	$GDAS_{hs}$
$GDAS_{100}$	87%	86%	71%	70%
FNL_{100}	–	80%	67%	69%
$GDAS_{250}$		–	81%	69%
$GDAS_{700}$			–	63%

Table A2-3. Proportion of days in sectors for the sensitivity analysis of the year 2005. The multisector is all days not being classified into any of the four sectors.

Simulation	SW	SE	NW	NE	Multisector
$GDAS_{100}$	16%	6%	11%	9%	58%
FNL_{100}	19%	7%	12%	8%	54%
$GDAS_{250}$	16%	6%	12%	9%	57%
$GDAS_{700}$	18%	5%	12%	9%	56%
$GDAS_{hs}$	18%	7%	13%	8%	54%

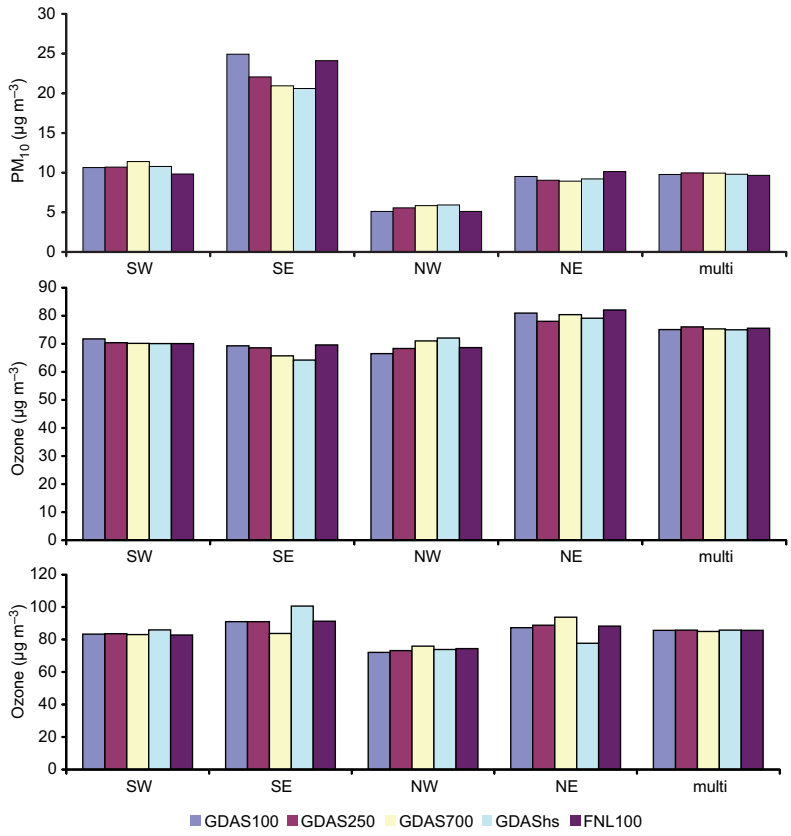

Fig. A2-1. Annual mean of PM_{10} (top); annual (middle), and March–September (bottom) means of daily maximum eight-hour ozone concentrations in air classified by sector based on trajectories from five sensitivity cases for 2005 (*see* Table A2-1).

seen in the southeastern source region where the average concentration decreased with increasing starting height; the annual average using 100-m trajectory as a starting height for the back-trajectory was 13% and 19% higher as compared with the values obtained for 250 and 700 m heights, respectively. There was only little difference in the annual average of daily maximum eight-hour ozone concentrations between the sensitivity runs (for the southeast, the 100-m annual average ozone concentration was 1% and 5% higher than those for 250-m and 700-m arrival heights, respectively, and for the northwest the average at 100-m was 3% and 6% lower than those at the 250-m and 700-m arrival heights, respectively). The most suitable starting height for this study could not be decided from these results, but while it is clear that different starting heights affect the results, they do not change the overall conclusions of this study.

Also changing horizontal starting position to a different grid point led to some changes in average concentrations (17% decrease for PM_{10} and 7% decrease for ozone for the southeastern source region). The hourly source-region classification agreement for the two positions was only 70%. Had the starting height been set much higher in the atmospheric boundary layer, the differences would probably have been smaller as the effect of the wind due to topographic differences, would have decreased. Also in this case, the overall conclusions of the study do not change with choice of horizontal starting location.

The increased resolution of the GDAS dataset as compared with that of the earlier FNL resulted in a 13% change in the source-region distribution, but also here average PM_{10} and ozone concentrations were very similar. The differences between GDAS and FNL are partly due to wind speed interpolation and wind field errors. Although we assumed that GDAS produces more accurate trajectories, the sensitivity analysis indicates that for the studied period, both datasets produced similar and comparable results.

Appendix 3. Top panel: Surface ozone (red) and PM_{10} (blue) for the period from midnight 28 April to midnight 14 May 2006. The dashed line is the 120 μg m^{-3} ozone threshold limit for daily maximum eight-hour average ozone. Unit: μg m^{-3}. Middle left two panels: hourly backward trajectories for the two days in the period with highest observed daily mean PM_{10} concentration. Two middle right panels and all bottom panels: Eight hourly backward trajectories giving rise to daily maximum eight-hour mean surface ozone for the six days in the period that exceeded the 120 μg m^{-3} ozone threshold limit.